

Finite Element, Discontinuous Galerkin, and Finite Difference Evolution Schemes in Spacetime

G Zumbusch

Institut für Angewandte Mathematik, Friedrich-Schiller-Universität Jena,
07743 Jena, Germany

E-mail: gerhard.zumbusch@uni-jena.de

Abstract. Numerical schemes for Einstein's vacuum equation are developed. Einstein's equation in harmonic gauge is second order symmetric hyperbolic. It is discretized in four-dimensional spacetime by Finite Differences, Finite Elements, and Interior Penalty Discontinuous Galerkin methods, the latter related to Regge calculus. The schemes are split into space and time and new time-stepping schemes for wave equations are derived. The methods are evaluated for linear and non-linear test problems of the Apples-with-Apples collection.

PACS numbers: 04.25.D, 02.70.Bf, 02.70.Dh, 04.20.Fy

1. Introduction

Numerical methods for the solution of Einstein's equation in general relativity are mainly based on Finite Differences (FD) and Pseudo-Spectral-Collocation (Bonazzola et al. 2004, Boyle et al. 2007) schemes space so far. The Finite Element method (FEM), or more generally Galerkin schemes have been used for reduced or auxiliary problems in numerical relativity (Arnold et al. 1998, Metzger 2004, Sopena et al. 2006, Aksoylu et al. 2008, Field et al. 2009). However, Galerkin methods are heavily used for the solution of wave problems in areas like acoustic and electro-magnetic scattering and elastic waves (Cohen 2002). This is mainly due to their way to deal with heterogeneous media and arbitrarily shaped geometric objects, represented by unstructured grids. Furthermore, the convergence theory of Galerkin methods is based on lower regularity (differentiability) requirements than Finite Differences and spectral methods.

General relativity is governed by Einstein's equation, which can be written as a system of second order partial differential equations in spacetime. In order to define a well-posed initial-value (Cauchy) problem, additional gauge conditions are needed. For the numerical solution of the system, spacetime is usually split into space and time $3+1$ and finally a time-stepping scheme is derived. Using a lapse- and a shift-function, a sequence of space-like manifolds is constructed, which fixes the gauge freedom. There are many improvements of the original ADM (Arnowitt et al. 1962, York 1979) splitting like BSSN (Shibata & Nakamura 1995, Baumgarte & Shapiro 1999). The equations are

usually discretized in space by FD or spectral schemes and independently in time by an explicit integrator for ordinary differential equations.

The harmonic approach and its generalizations first incorporate the harmonic gauge condition into Einstein's equation in spacetime to derive a hyperbolic system (Fock 1959, Bruhat 1962, Reula 1998, Friedrich & Rendall 2000, Pretorius 2005). Afterwards, the system is again split into space and time and discretized. Generalized harmonic methods modify the gauge condition, but usually preserve the hyperbolicity.

In this paper, we follow a slightly different approach. Starting with the hyperbolic system of Einstein's equation in harmonic gauge, we discretize first in spacetime. Introducing a global time-step, the system is split afterwards in space and time. However, adaptive grid refinement in space and local time-stepping schemes can also be derived in a consistent way. This is similar to Regge calculus (Regge 1961, Sorkin 1975) in spacetime.

The main contribution of the paper however is the development of a Finite Element and an Interior Penalty Discontinuous Galerkin (DG) method for Einstein's vacuum equation. Both methods are derived from a variational formulation, which is obtained from the Einstein-Hilbert action and harmonic gauge. In fact, Galerkin methods are always based on a variational version of the differential equations.

Galerkin schemes have been considered for the discretization of wave equations in several ways so far: The wave equation $\partial_{tt}u = \Delta u$ as an example problem is written in variational form as

$$\int_{\Omega} (\partial_{tt}u) w d^3x = - \int_{\Omega} (\nabla u) \cdot (\nabla w) d^3x \quad \forall w$$

with trial functions w , integration over the spatial domain Ω , and zero boundary conditions. This gives rise to FEM (Dupont 1973, Baker & Bramble 1979) and DG (Ainsworth et al. 2006, Grote et al. 2006, Field et al. 2009) in space schemes, used in conjunction with a standard time integrator like the leapfrog scheme. The first order in time formulation $\partial_t v = \Delta u$ and $\partial_t u = v$ in variational version in time reads as

$$\begin{aligned} - \int_T v (\partial_t w) dt &= \int_T (\Delta u) w dt \quad \forall w \\ - \int_T u (\partial_t w) dt &= \int_T v w dt \quad \forall w \end{aligned}$$

on the interval T and without initial value terms. In order to obtain a time-stepping scheme, a time-discontinuous Galerkin method can be constructed (Jamet 1978, Eriksson et al. 1985). Note that time continuous functions do not lead to a time-stepping scheme, but a single large equation system for all times. We can combine both Galerkin schemes to a spacetime FEM like

$$\begin{aligned} \int_{\Omega \times T} v (\partial_t w) dt d^3x &= \int_{\Omega \times T} (\nabla u) \cdot (\nabla w) dt d^3x \quad \forall w \\ - \int_{\Omega \times T} u (\partial_t w) dt d^3x &= \int_{\Omega \times T} v w dt d^3x \quad \forall w, \end{aligned}$$

continuous (French & Peterson 1996, Anderson & Kimn 2007) and discontinuous (Hulbert & Hughes 1990, Monk & Richter 2005) in time. In this paper, however, we will consider second order in space and time formulations of type

$$\int_{\Omega \times T} (\partial_{tt}u) (\partial_t w) dt d^3x = \int_{\Omega \times T} (\nabla u) \cdot (\nabla w) dt d^3x \quad \forall w, \quad (1)$$

again without boundary and initial value terms. It can be re-written covariant and leads to time-stepping algorithms even for time-continuous Galerkin discretizations, which differ from first order formulations in general.

The first result of the paper in section 2 is in fact the derivation of such a variational formulation of Einstein's equation from the Einstein-Hilbert action. In addition, a linearized formulation is discussed.

If we restrict the solution and trial functions in (1) to some finite dimensional spaces, we obtain Galerkin discretizations in section 3. Although the spacetime formulation relates values at different points in space and time, it reduces to a time-stepping scheme for global time steps. The FEM scheme reduces further to the leapfrog time-stepping for piecewise linear functions in time, equidistant time steps, and without mixed space-time-derivatives. Note that leapfrog is related to the Störmer-Verlet scheme and a special case of the Newmark scheme. However, in the general spacetime case the FEM and the symmetric and non-symmetric DG spacetime schemes seem to be new. They form the next result of this paper, see sections 3.3 and 3.4.

While the leapfrog scheme is explicit for FD in space, see (Cohen 2002) and (Pretorius 2005, App. B), the FEM method in space requires the solution of a global equation system with mass matrix $\int_{\Omega} uw d^3x$ each time step. The DG method in space is computationally more efficient than FEM in general, because the mass matrix is block-diagonal and the equation systems are easier to solve. However, by a special choice of numerical quadrature rules (mass-lumping) in FEM, see (Cohen 2002), and a choice of orthogonal ansatz functions in DG, see (Rivière 2008), the mass matrix is diagonal and the equation systems are trivial to solve.

Now we put together the variational formulation of Einstein's equation and the spacetime Galerkin schemes and we obtain in section 3.6, as the main result, a FEM, a symmetric and a non-symmetric Interior Penalty DG method for Einstein's full vacuum equation. As an intermediate step we briefly discuss a simpler, linearized version of Einstein's equation.

Memory requirements for nodal FD and piecewise linear FEM schemes for Einstein's equation are comparable, namely ten metric component values per grid node. The DG methods need this storage of 10 values for each element and each ansatz function, i.e. $10 \cdot 5$ or $10 \cdot 16$ for linear or multi-linear functions, thus are more memory intensive. The fields are needed for two previous and the current time-slice in the leapfrog time-stepping. We put the discrete fields into the variational formulation, which now translates to non-linear equation systems. The matrix entries are computed by numerical quadrature rules. Additional storage may be required for the matrices and solution of the equation systems, which depends on the solver.

Finally, some numerical experiments inspired by the Apples-with-Apples test suite (Alcubierre et al. 2004, Babiuc et al. 2008) are used to compare both schemes with a more traditional FD scheme in section 4. The Galerkin schemes with piecewise linear functions on equidistant, cartesian grids show comparable CFL conditions, comparable second order accuracy, similar (sometimes opposite sign) dispersion second order in

grid spacing, and comparable second order accurate harmonic gauge conditions. The errors on unstructured grids additionally depend on the orientation of the elements with respect to the wave characteristics and element angle conditions.

In order to solve realistic test cases in general relativity, techniques to handle apparent horizons are needed. Standard techniques include the puncture approach (Brandt & Bruegmann 1997, Campanelli et al. 2006, Baker et al. 2006), excision (Pretorius 2005), and singularity avoiding slicing conditions. Slicing would lead to a generalized harmonic gauge. Excision is compatible with harmonic gauge and the excised domain can be approximated by unstructured grids, which seems to be most promising. Furthermore, the Galerkin schemes have to be generalized to higher order, which is straightforward in space, but is more difficult in time for stability reasons.

2. Einstein's Vacuum Equation

2.1. Strong Formulation

We start with the standard derivation of Einstein's equation via the Einstein-Hilbert action defined by

$$S := \int_{\mathcal{M}} R \sqrt{-g} d^4x$$

in the case of vacuum, in the notation of (Straumann 2004). We consider it as a function of the metric tensor $g_{\alpha\beta}$ and its derivatives. The Ricci tensor $R_{\alpha\beta}$ and the Ricci scalar $R = g^{\alpha\beta} R_{\alpha\beta}$ contain up to second order partial derivatives of $g_{\alpha\beta}$. We are looking for an extremum of S . The variation of S is

$$\delta S = \int_{\mathcal{M}} (R_{\mu\nu} - \frac{1}{2} g_{\mu\nu} R) (\delta g^{\mu\nu}) \sqrt{-g} d^4x, \quad (2)$$

as long as the variation $\delta g^{\mu\nu}$ vanishes at the boundary of the domain \mathcal{M} . Otherwise we obtain an additional boundary term

$$\frac{3}{2} \int_{\partial\mathcal{M}} g^{\alpha\beta} g^{\mu\nu} (\partial_\nu \delta g_{\mu\beta} - \partial_\beta \delta g_{\mu\nu}) n_\alpha^{(g)} d^3x \quad (3)$$

which can be used later for boundary conditions using derivatives of $g_{\mu\nu}$. We rename the variation

$$v^{\mu\nu} := \delta g^{\mu\nu}.$$

The variational formulation reads as: We seek a solution $g_{\alpha\beta} \in V_a$ such that $\delta S = 0$ for all $v_{\alpha\beta} \in V_t$ with appropriate ansatz and trial spaces. Dirichlet boundary conditions on (parts of) $\partial\mathcal{M}$ can be built into V_a and V_t : The solution takes the Dirichlet values and the trial functions vanishes there. Boundary conditions involving derivatives require an additional boundary term like (3). The variational formulation translates to the strong formulation as $R_{\mu\nu} - \frac{1}{2} g_{\mu\nu} R = 0$ or in vacuum

$$R_{\mu\nu} = 0$$

with appropriate boundary conditions. However, in order to obtain a well posed initial-boundary-value or Cauchy problem, we need an additional gauge condition. We choose the standard harmonic gauge with

$$\Gamma^\alpha := g^{\rho\sigma} \Gamma_{\rho\sigma}^\alpha = 0 , \quad (4)$$

which is a condition on first order derivatives of $g_{\alpha\beta}$. This way, we can modify Einstein's equation as

$$R_{\mu\nu}^{(h)} := R_{\mu\nu} - \frac{1}{2} g_{\alpha\nu} \partial_\mu \Gamma^\alpha - \frac{1}{2} g_{\alpha\mu} \partial_\nu \Gamma^\alpha = 0 , \quad (5)$$

with principal part

$$R_{\mu\nu}^{(h)pp} := -\frac{1}{2} g^{\alpha\beta} \partial_\alpha \partial_\beta g_{\mu\nu} . \quad (6)$$

Now, we have a quasi-linear, second order, symmetric hyperbolic differential equation, which we will later discretize by finite differences. Note that this remains true if we switch to a generalized harmonic gauge. Equation (4) changes to $\Gamma^\alpha = H^\alpha(x, g)$ with a gauge driver H . This driver may depend on coordinates and the metric, but must be independent of derivatives of g in order to preserve the principal part $R^{(h)pp}$.

2.2. Variational Formulation

Galerkin discretizations are based on a variational formulation. We start with the standard variational formulation (2). By Stokes' theorem, we can remove the second order derivatives. With harmonic gauge (4) we arrive at a variational version of (6)

$$a(g, v) := \frac{1}{2} \int_{\mathcal{M}} g^{\alpha\beta} \sqrt{-g} (\partial_\alpha g_{\mu\nu}) (\partial_\beta v^{\mu\nu}) d^4x , \quad (7)$$

which is symmetric in the first order derivatives of $g_{\mu\nu}$ and $v^{\mu\nu}$ in the special case of a fixed background $g^{\mu\nu}$. Again there is an additional boundary term, if the variation v does not vanish on the boundary $\partial\mathcal{M}$

$$- \frac{1}{2} \int_{\partial\mathcal{M}} g^{\alpha\beta} \sqrt{-g} (\partial_\beta g_{\mu\nu}) v^{\mu\nu} n_\alpha^{(g)} d^3x . \quad (8)$$

The remaining terms can be assembled in

$$\begin{aligned} q(g, v) := \frac{1}{2} \int_{\mathcal{M}} g^{\alpha\beta} g^{\rho\sigma} \sqrt{-g} \Big(& (\partial_\alpha g_{\rho\mu}) (\partial_\beta g_{\sigma\nu}) - (\partial_\alpha g_{\rho\mu}) (\partial_\sigma g_{\beta\nu}) \\ & + (\partial_\alpha g_{\rho\mu}) (\partial_\nu g_{\beta\sigma}) + (\partial_\mu g_{\alpha\rho}) (\partial_\beta g_{\sigma\nu}) \\ & - \frac{1}{2} (\partial_\mu g_{\alpha\rho}) (\partial_\nu g_{\beta\sigma}) \Big) v^{\mu\nu} d^4x , \end{aligned} \quad (9)$$

which is quadratic and symmetric in the first order derivatives of $g_{\mu\nu}$, compare also (Fock 1959, App. B). The variational formulation now reads as

$$\begin{aligned} \text{seek } g \in V_a \text{ such that } a(g, v) + q(g, v) &= 0 \quad \forall v \in V_t \\ \text{and } \Gamma^\alpha &= 0 . \end{aligned} \quad (10)$$

Note that metric $g \in V_a$ in (10) does not need to have well defined second derivatives as in (5) and may be chosen in an appropriate Sobolev space. In the case of a non vanishing energy-momentum tensor $T^{\mu\nu}$ additional terms of type

$$b(g, v) := \int_{\mathcal{M}} (g_{\alpha\nu} g_{\mu\beta} - \frac{1}{2} g_{\mu\nu} g_{\alpha\beta}) \sqrt{-g} T^{\alpha\beta} v^{\mu\nu} d^4x$$

appear on the right-hand side of (10).

Different types of initial and boundary conditions can be imposed on $\partial\mathcal{M}$ by standard procedures to define a Cauchy problem: Homogeneous Dirichlet values are directly incorporated into all functions in V_a and V_t . Inhomogeneous Dirichlet conditions are built into the solution g , either direct in the discrete numerical scheme, or via an additive splitting into a homogeneous auxiliary solution and a non-homogeneous function for the boundary conditions. Neumann boundary conditions and other conditions based on derivatives of the solution on parts of $\partial\mathcal{M}$ lead to additional terms in a of type (8), where $\partial_\beta g_{\mu\nu}$ is replaced by the given derivatives. The functions in V_a and V_t do not vanish there. “Natural” boundary conditions can be defined as vanishing term (8), that is $g^{\alpha\beta} \sqrt{-g} (\partial_\beta g_{\mu\nu}) n_\alpha^{(g)} = 0$. The conditions can be translated back into a strong formulation via (3).

2.3. Linearized Equations

In a weak field approximation of Einstein’s equation, we neglect the first order derivatives in (5) and arrive at $R_{\mu\nu}^{(h)pp} = 0$ for some background metric $\hat{g}^{\mu\nu}$. In the variational version (10), we can neglect $q(g, v)$ and solve for $a(g, v) = 0$ instead, again for a fixed background metric $\hat{g}^{\mu\nu}$.

$$a(g, v) := \frac{1}{2} \int_{\mathcal{M}} \hat{g}^{\alpha\beta} \sqrt{-\hat{g}} (\partial_\alpha g_{\mu\nu}) (\partial_\beta v^{\mu\nu}) d^4x \quad (11)$$

The linearized version of the harmonic gauge condition (4) reads

$$\hat{g}^{\alpha\beta} \hat{g}^{\mu\nu} (\partial_\mu g_{\nu\beta} - \frac{1}{2} \partial_\beta g_{\mu\nu}) = 0 . \quad (12)$$

Now, we simplify the equations even further and consider a weak field in flat space. The linearization is taken around Minkowski metric $\hat{g} = \eta := \text{diag}(-1, 1, 1, 1)$ and we obtain the strong formulation

$$-\frac{1}{2} \square g_{\mu\nu} = 0 \quad (13)$$

with $\partial^\alpha = \eta^{\alpha\beta} \partial_\beta$ and $\square = \partial^\alpha \partial_\alpha$. This translates to the variational version

$$\text{seek } g \in V_a \text{ such that } a(g, v) := \frac{1}{2} \int_{\mathcal{M}} \eta^{\alpha\beta} (\partial_\alpha g_{\mu\nu}) (\partial_\beta v^{\mu\nu}) d^4x = 0 \quad \forall v \in V_t . \quad (14)$$

The harmonic gauge condition (12) reduces to

$$\partial^\mu g_{\mu\nu} - \frac{1}{2} \eta_{\mu\nu} \eta^{\alpha\beta} \partial^\mu g_{\alpha\beta} = 0 ,$$

which can be further simplified by the substitution $h_{\mu\nu} := g_{\mu\nu} - \frac{1}{2} \eta^{\alpha\beta} g_{\alpha\beta}$ to

$$\partial^\mu h_{\mu,\nu} = 0 . \quad (15)$$

The differential equation still is (13) $-\frac{1}{2}\square h_{\mu\nu} = 0$, now with a divergence free h . The gauge conditions are linear and can be incorporated into the spaces V_a and V_t .

3. Numerical Schemes

3.1. Finite Differences (FD)

For illustration purposes, the first numerical spacetime scheme will be based on finite differences. We consider the discretization of a linear, scalar, second order wave equation $-\square u = 0$ with suitable initial and boundary conditions. On a one-dimensional, equidistant grid with grid spacing h , we choose the stencil $(u(x-h)-2u(x)+u(x+h))/h^2$, also abbreviated as $[1 \ -2 \ 1]/h^2$, to approximate the second derivative. It is second order accurate for u smooth enough. The d'Alembert operator can be obtained by an application of the stencil along each coordinate axis on a cartesian grid. The two dimensional stencil at a grid point (i, j) for example is

$$\frac{u_{i-1,j} - 2u_{i,j} + u_{i+1,j}}{h_0^2} - \frac{u_{i,j-1} - 2u_{i,j} + u_{i,j+1}}{h_1^2} = 0 ,$$

which gives the explicit time stepping scheme

$$u_{i+1,j} = 2u_{i,j} - u_{i-1,j} + \left(\frac{h_0}{h_1}\right)^2 (u_{i,j-1} - 2u_{i,j} + u_{i,j+1})$$

using values at time slices $i-1$ and i to calculate the values at time slice $i+1$. This is the leapfrog scheme in time and can be written as

$$u_{i+1} = 2u_i - u_{i-1} + (h_0)^2 \Delta_h u_i \quad (16)$$

with a FD approximation of the spatial derivatives Δ . Note that a CFL condition $h_0/h_k < 1$ for all $k > 0$ must hold for stability reasons (Cohen 2002). The initial conditions can be prescribed at two times slices $x_0 = 0$ and $x_0 = h_0$, the boundary values at $x_k = 0$ and $x_k = 1$. Modifications for other types of initial and boundary conditions do exist.

3.2. Compact Finite Difference Stencils (FDM)

In order to generalize the FD stencils to mixed first and second order derivatives, we consider an alternative construction. In the one dimensional case, first derivatives can be approximated by central stencils $u'(x+h/2) \approx (u(x+h) - u(x))/h$ at grid points $x+h/2$. The second derivative can be calculated as a central stencil of first derivatives $u''(x) \approx (u'(x+h/2) - u'(x-h/2))/h$ which reduces to the one-dimensional FD stencil. However, in two (and more) dimensions the construction differs, if we consider cell-centered first derivatives: We differentiate in one directions and average in the other direction(s):

$$\partial_0 u_{i+1/2,j+1/2} \approx \frac{1}{2} \left(\frac{u_{i-1,j} - u_{i,j}}{h_0} + \frac{u_{i-1,j+1} - u_{i,j+1}}{h_0} \right) .$$

We obtain the second derivatives as stencils

$$\partial_0 \partial_0 \approx \frac{1}{(2h_0)^2} \begin{bmatrix} -1 & 2 & -1 \\ -2 & 4 & -2 \\ -1 & 2 & -1 \end{bmatrix} \text{ and } \partial_0 \partial_1 \approx \frac{1}{4h_0 h_1} \begin{bmatrix} -1 & 0 & 1 \\ 0 & 0 & 0 \\ 1 & 0 & -1 \end{bmatrix} .$$

The discretization of the d'Alembert operator again gives a time-stepping scheme for time slice $i + 1$. However, the scheme is no more explicit like (16). Let us write the difference stencil $[1 \ 2 \ 1]/4$ as the matrix M and the stencil $[-1 \ 2 \ -1]/(h_1)^2$ as matrix A . We obtain the scheme

$$Mu_{i+1} = 2Mu_i - Mu_{i-1} - (h_0)^2 Au_i . \quad (17)$$

We can compute the values u_{i+1} at time slice $i + 1$ by the solution of a linear equation system with matrix M using the values u_i and u_{i-1} at time slices i and $i - 1$. The matrix is positive definite, symmetric, and of bounded condition number. Hence, the system is easy to solve numerically for large systems by standard iterative solvers. Again, the CFL condition limits the time step size h_0 .

3.3. Finite Element and Petrov-Galerkin Methods (FEM)

We start with a variational version of the d'Alembert operator (1), a first step towards (11):

$$\frac{1}{2} \int_{\mathcal{M}} \eta^{\alpha\beta} (\partial_\alpha u) (\partial_\beta v) d^4x = 0 \quad \forall v \quad (18)$$

Following standard procedures in FEM, we choose a set of global, continuous, piecewise polynomial ansatz and trial functions $\tilde{\phi}_i \in V_a$ and $\tilde{\psi}_j \in V_t$ as a basis of finite dimensional spaces V_a and V_t , and obtain a finite element method: Find the coefficients \tilde{u}_i of the solution $u = \sum_i \tilde{u}_i \phi_i \in V_a$, such that (18) holds for all trial functions $v \in V_t$. This can be written in basis functions as

$$\frac{1}{2} \sum_i \tilde{u}_i \int_{\mathcal{M}} \eta^{\alpha\beta} (\partial_\alpha \tilde{\phi}_i) (\partial_\beta \tilde{\psi}_j) d^4x = 0 \quad \forall j \quad (19)$$

and in matrix notation $\tilde{A}\tilde{u} = 0$ with solution vector \tilde{u} and matrix $\tilde{A} = (\tilde{a}_{ij})$

$$\tilde{a}_{ij} = \frac{1}{2} \int_{\mathcal{M}} \eta^{\alpha\beta} (\partial_\alpha \tilde{\phi}_i) (\partial_\beta \tilde{\psi}_j) d^4x .$$

This is a spacetime discretization. Introducing a global time step, we split functions $\tilde{\phi}_i(x) = \phi_i^0(x_0)\phi_i^s(x_1, x_2, x_3)$ and $\tilde{\psi}_j$, and the domain $\mathcal{M} = T \times \Omega$ into time and space. Further, mixed space-time derivatives $\eta^{a0} = \eta^{0b} = 0$ do not occur with space index a, b . We obtain

$$\begin{aligned} \tilde{a}_{ij} &= \frac{1}{2} \left(\int_T \eta^{00} (\partial_0 \phi_i^0) (\partial_0 \psi_j^0) dt \right) \left(\int_\Omega \phi_i^s \psi_j^s d^3x \right) \\ &+ \frac{1}{2} \left(\int_T \phi_i^0 \psi_j^0 dt \right) \left(\int_\Omega \eta^{ab} (\partial_a \phi_i^s) (\partial_b \psi_j^s) d^3x \right) . \end{aligned}$$

We introduce the mass matrix M and matrix A by

$$\begin{aligned} m_{ij} &= \frac{1}{2} \int_\Omega \phi_i^s \psi_j^s d^3x \text{ and} \\ a_{ij} &= \frac{1}{2} \int_\Omega \eta^{ab} (\partial_a \phi_i^s) (\partial_b \psi_j^s) d^3x . \end{aligned}$$

In order to solve a Cauchy problem with initial conditions, we deviate from standard FEM for self-adjoint problems in a single detail: In order to mimic the behavior of the spacetime FD schemes, we start with initial data at two time slices $i - 1$ and i and use the scheme to calculate the next time slice $i + 1$. We use piecewise linear functions $\phi_i^0(t) = \max(1 - |t - x_i|/h_0, 0)$ and ψ_j^0 in time for equidistant time-steps h_0 and obtain the system in time $\frac{1}{h_0}[-1 \ 2 \ -1]M + \frac{h_0}{6}[1 \ 4 \ 1]A$, which is of leapfrog type

$$\left(M - \frac{h_0^2}{6}A\right) u_{i+1} = \left(M + \frac{2h_0^2}{3}A\right) u_i - \left(M - \frac{h_0^2}{6}A\right) u_{i-1}. \quad (20)$$

In the $1 + 1$ spacetime case, piecewise linear functions on an equidistant space grid, we further obtain $M = \frac{h_1}{6}[1 \ 4 \ 1]$ and $A = \frac{1}{h_1}[-1 \ 2 \ -1]$.

The method can be interpreted as a Petrov-Galerkin method with different ansatz V_a and trial V_t spaces: We use piecewise polynomial functions centered at a grid point i at time i_0 and space location (i_1, i_2, i_3) for a cartesian grid. The functions are chosen piecewise linear in time. Let the grid points be in the time domain $(0, k)$ with initial conditions at $i_0 = 0$ and $i_0 = 1$. We compute the solution for all ansatz functions ϕ_i located at times $(2, k)$. However, we choose the trial functions ψ_j located at times $(1, k - 1)$. The trial functions lag behind one time slice, but are identical in space. This is exactly the idea to solve for the next time slice $i_0 + 1$ and coincides with a leapfrog scheme for equidistant time steps.

The solution of equation systems is the most expensive part of the time stepping procedure. The advantage of FD schemes for leapfrog (16) is that mass matrix M is the identity and no equation systems have to be solved. However, there is a common technique in FEM called “mass lumping” to obtain diagonal matrices M , too: Integration in terms of type $\int_{\Omega} \phi_i^s \phi_j^s d^3x$ and $\int_T \phi_i^0 \phi_j^0 dt$ are approximated by numerical quadrature rules on each finite element. For piecewise (multi-) linear functions, quadrature rules prove to be sufficient, which are based on the function values at the element vertices only. This is the trapezoidal rule on an edge and its generalizations to rectangles, cubes, triangles and tetrahedra. The ansatz functions fulfill $\phi_i^s(x_j) = \delta_{ij}$ and the mixed products $(\phi_i^s \phi_j^s)(x_k) = \delta_{ik} \delta_{jk} = 0$ for $i \neq j$ vanish on all element vertices x_k . Hence, off-diagonal entries m_{ij} vanish and M is in fact a diagonal matrix. We arrive at the computational efficiency of an FD scheme (16), once the integration is done.

Note that (19) defines spacetime FEM also for higher order methods in space by piecewise polynomial functions ϕ_i^s and ψ_j^s , by pseudo-spectral Galerkin schemes in space, on unstructured grids in spacetime, and for adaptive grid refinement in spacetime. The approach does not easily extend to higher order methods in time due to a lack of stability of the respective time-stepping schemes.

3.4. Interior Penalty Discontinuous Galerkin Methods (DG)

Again, we start with the variational problem (18). However, we choose piecewise polynomial ansatz and trial functions ϕ_i and ψ_j , which are no longer continuous over element boundaries. This leads to additional terms. Consider a common face

$e_{ij} := \partial E_i \cap \partial E_j$ of two neighbor elements E_i and E_j and normal unit vector n^{ij} oriented from E_i to E_j . We denote the average by $\{u\} := ((u|_{E_i}) + (u|_{E_j}))/2$ and the jump by $[u] := (u|_{E_i}) - (u|_{E_j})$ on the face e_{ij} . Let the volume of the face be $|e_{ij}|$. We split the integration over \mathcal{M} of (14) into the integration over elements E_i and all faces e_{ij} of the grid.

$$\begin{aligned} a(u, v) &:= \frac{1}{2} \sum_i \int_{E_i} \eta^{\alpha\beta} (\partial_\alpha u) (\partial_\beta v) d^4x \\ &\quad - \frac{1}{2} \sum_{i < j} \int_{e_{ij}} \{ \eta^{\alpha\beta} n_\alpha^{ij} \partial_\beta u \} [v] d^3x \\ &\quad - \frac{1}{2} \sum_{i < j} \int_{e_{ij}} [u] \{ \eta^{\alpha\beta} n_\alpha^{ij} \partial_\beta v \} d^3x \\ &\quad + \frac{1}{2} \sum_{i < j} \frac{c_p}{|e_{ij}| c_e} \eta^{\alpha\beta} n_\alpha^{ij} n_\beta^{ij} \int_{e_{ij}} [u] [v] d^3x = 0 \end{aligned} \tag{21}$$

The first jump term is obtained by Stokes' theorem, the second is added for reasons of symmetry of a , and the last term with penalty parameters c_p and c_e weakly imposes inter-element continuity. We have modified the penalty term, originally strictly positive for elliptic operators, by $\{\eta^{\alpha\beta} n_\alpha^{ij} n_\beta^{ij}\}$ due to the indefiniteness of the bi-linear form.

We choose polynomial ansatz and trial functions on each element and combine them without continuity to global functions ϕ_i and ψ_j . They define a basis of the finite dimensional spaces V_a and V_t . Find coefficients \tilde{u}^i such that

$$\sum_i \tilde{u}^i a(\phi_i, \psi_j) = 0 \quad \forall j.$$

The scheme is called the symmetric interior penalty discontinuous Galerkin scheme (SIPDG). Note that an opposite sign of the second jump term leads to the alternative non-symmetric NIPDG scheme, in our case with penalty $c_p = 0$. Boundary conditions require modifications of the terms with outer boundary faces, see (Rivière 2008).

If we use linear polynomials along each coordinate axis on an equidistant grid as before, we can calculate the difference stencils explicitly. In two dimensions $n = 2$ for example, we use the local nodal basis $(1 - x_0)(1 - x_1)$, $x_0(1 - x_1)$, $(1 - x_0)x_1$, x_0x_1 and shift and scale it to each element. Again we solve for time slice $i + 1$ using slices $i - 1$ and i . However, now there are four degrees of freedom per element instead of one per node. With a penalty term $c_e = 1$ and different constants c_p in both directions, we obtain

$$\begin{aligned} A_{1,0} = A_{-1,0}^* &= \frac{h_1}{12h_0} \begin{pmatrix} 2 & 1 & 0 & 0 \\ 1 & 2 & 0 & 0 \\ -4 & -2 & 2 & 1 \\ -2 & -4 & 1 & 2 \end{pmatrix} + \frac{c_{p1}}{6} \begin{pmatrix} 0 & 0 & 0 & 0 \\ 0 & 0 & 0 & 0 \\ 2 & 1 & 0 & 0 \\ 1 & 2 & 0 & 0 \end{pmatrix} \\ A_{0,-1} = A_{0,1}^* &= \frac{h_0}{12h_1} \begin{pmatrix} 2 & -4 & 1 & -2 \\ 0 & 2 & 0 & 1 \\ 1 & -2 & 2 & -4 \\ 0 & 1 & 0 & 2 \end{pmatrix} + \frac{c_{p0}}{6} \begin{pmatrix} 0 & 2 & 0 & 1 \\ 0 & 0 & 0 & 0 \\ 0 & 1 & 0 & 2 \\ 0 & 0 & 0 & 0 \end{pmatrix} \\ A_{0,0} &= -\frac{c_{p0}h_1}{6} \begin{pmatrix} 2 & 0 & 1 & 0 \\ 0 & 2 & 0 & 1 \\ 1 & 0 & 2 & 0 \\ 0 & 1 & 0 & 2 \end{pmatrix} + \frac{c_{p1}h_0}{6} \begin{pmatrix} 2 & 1 & 0 & 0 \\ 1 & 2 & 0 & 0 \\ 0 & 0 & 2 & 1 \\ 0 & 0 & 1 & 2 \end{pmatrix} \end{aligned}$$

and a 5-block scheme for the degrees of freedom in element at time $i + 1$ and position j

$$A_{1,0}u_{i+1,j} = A_{0,-1}u_{i,j-1} + A_{0,0}u_{i,j} + A_{0,1}u_{i,j+1} - A_{-1,0}u_{i-1,j} . \quad (22)$$

Note that for each element a linear equation system $A_{1,0}$ needs to be solved. It is of the size of number of ansatz functions, which is cheaper to solve than the single large equation system for the FEM. However, the amount of work can be further reduced: It is possible to choose the local ansatz functions orthogonal with respect to the bi-linear form such that $A_{1,0}$ is in fact diagonal or even the identity and no systems need to be solved any more. This way, we obtain an explicit time-stepping scheme like (16).

For a second order differential equation in time, we need two initial conditions, like $u(0, x_1)$ and $\partial_0 u(0, x_1)$. This can be converted into data on two initial time slices $i = 0$ and $I01$. However, for the DG schemes, we need an initial spacetime approximation in elements at times slices 0 and 1. For a linear ansatz in time direction, initial data is needed at least at the beginning and end of both time slices, namely three initial values. These can be computed with a start-up calculation.

3.5. Linearized Einstein's Equation

In order to solve linearized Einstein's equation (13) resp. (14), we can generalize the scalar schemes for $\square u$, apply these to each component $g_{\mu\nu}$, and set the background metric to Minkowski $\hat{g} = \eta$. The linear gauge condition (15) needs to be fulfilled. Divergence-free initial data guarantees this for all times in the continuous case. However, numerical errors will lead to a violation of the gauge condition. DG methods easily allow for locally divergence-free ansatz functions on each element. In contrast, it is difficult to implement globally divergence-free symmetric tensor fields in FEM analogous to divergence-free vector fields for Maxwell's equation, see (Nedelec 1980, Nedelec 1986).

In the case of a prescribed curved background metric, we have to solve the linear, variable coefficient problem $R_{\mu\nu}^{(h)pp} = 0$. The FD stencils are no longer applicable and we switch to the compact FDM stencils. The FEM implementation is based on the variational formulation

$$\frac{1}{2} \sum_i u^i \int_{\mathcal{M}} \hat{g}^{\alpha\beta} \sqrt{-\hat{g}} (\partial_\alpha \phi_i) (\partial_\beta \psi_j) d^4x = 0 \quad \forall j . \quad (23)$$

The DG method now reads as

$$\begin{aligned} a(u, v) &:= \frac{1}{2} \sum_i \int_{E_i} \hat{g}^{\alpha\beta} \sqrt{-\hat{g}} (\partial_\alpha u) (\partial_\beta v) d^4x \\ &\quad - \frac{1}{2} \sum_{i < j} \int_{e_{ij}} \{ \hat{g}^{\alpha\beta} \sqrt{-\hat{g}} n_\alpha^{ij} \partial_\beta u \} [v] d^3x \\ &\quad - \frac{1}{2} \sum_{i < j} \int_{e_{ij}} [u] \{ \hat{g}^{\alpha\beta} \sqrt{-\hat{g}} n_\alpha^{ij} \partial_\beta v \} d^3x \\ &\quad + \frac{1}{2} \sum_{i < j} \frac{c_p}{|e_{ij}|^{ce}} \int_{e_{ij}} \{ \hat{g}^{\alpha\beta} n_\alpha^{ij} n_\beta^{ij} \sqrt{-\hat{g}} \} [u][v] d^3x = 0 \end{aligned} \quad (24)$$

where we have generalized the penalty term to $\{ \hat{g}^{\alpha\beta} n_\alpha^{ij} n_\beta^{ij} \sqrt{-\hat{g}} \}$. The matrices M and A now depend on the background metric $\hat{g}^{\alpha\beta} \sqrt{-\hat{g}}$, which varies in spacetime. Procedures to construct a diagonal M like mass-lumping in FEM in section 3.3 and orthogonal ansatz functions in DG in in section 3.4 have to be performed on a per-element basis and are thus more expensive, as are procedures to construct divergence-free ansatz

spaces. Once the matrix entries have been computed, the linear equations system of type (20) and (22) can be solved by standard solvers.

3.6. Einstein's Vacuum Equation

We generalize the compact FDM stencils to Einstein's vacuum equation (5): The variable metric $g_{\mu\nu}$ and its second order derivatives $R_{\mu\nu}^{(h)}$ are chosen node centered (at grid points), but the first order derivatives $\Gamma_{\beta\gamma}^\alpha$ are chosen cell centered. The inverse metric $g^{\mu\nu}$ is used to calculate $\Gamma_{\beta\gamma}^\alpha$ and Γ^α and is also cell centered, defined as the inverse of the cell average of the metric $g_{\mu\nu}$. The products of averaged Γ enter the Ricci tensor, as well as the node centered derivatives of Γ . This way, we can use the standard formulas $\Gamma_{\beta\gamma}^\alpha := \frac{1}{2}g^{\alpha\sigma}(\partial_\beta g_{\gamma\sigma} + \partial_\gamma g_{\beta\sigma} - \partial_\sigma g_{\beta\gamma})$, $R_{\mu\nu} := \partial_\alpha \Gamma_{\mu\nu}^\alpha - \partial_\mu \Gamma_{\nu\alpha}^\alpha + \Gamma_{\alpha\beta}^\beta \Gamma_{\mu\nu}^\alpha - \Gamma_{\mu\alpha}^\beta \Gamma_{\nu\beta}^\alpha$, (4), and (5) to set up non-linear, discrete Einstein's equation and derive the time-stepping scheme. Note that no code generated by a symbolic algebra program is needed.

The FEM and DG Galerkin schemes can also be generalized to Einstein's equation. The form a (7) resp. (21) and the quadratic term q (9) define the variational problem (10a). The integration is done numerically. The integral $\int_{\mathcal{M}}$ is split into integrals over an element $\sum_i \int_{E_i}$ (and a face e_{ij} in (21)). The integrals over a single element E_i and face e_{ij} are approximated by a numerical quadrature rule. The integrands of a and q are evaluated at the quadrature points.

The matrices M and A now depend on the current metric $g^{\alpha\beta}\sqrt{-g}$ and the equation systems of type (20) and (22) are non-linear. The time-stepping schemes are implicit and require the solution of a non-linear equation system for each time-slice. The DG method leads to a set of easy to solve local equation systems for each element. The FDM and the FEM have global coupling of the degrees of freedom of a time slice. In both cases standard non-linear solvers can be used. Note that the explicit FD method both gives an initial guess for a locally fixed background metric $g^{\mu\nu}$ and can be used as a preconditioner for the principle part in an iterative solver.

The harmonic gauge condition (4) now is a non-linear condition and cannot be incorporated into a linear ansatz space V_a . Note that a change of variables leads to a formulation of Einstein's equation with a new metric $\mathbf{g}^{\mu\nu} := \sqrt{-g}g^{\mu\nu}$ and a linear gauge condition $\partial_\mu \mathbf{g}^{\mu\nu} = 0$, which could be built into V_a .

Note that Regge calculus also discretizes a variational principle in spacetime for simplicial grids (Sorkin 1975). It can be considered a DG spacetime scheme with piecewise constant metric tensor $g_{\mu\nu}$. This way, (21) generalizes it to higher order and arbitrary element shapes. However, Regge calculus does not use coordinates and is based on purely geometric entities like edge lengths and defect angles. Furthermore, the variation is with respect to the degrees of freedom, which are the squared edge lengths in Regge calculus and values of the metric in (21).

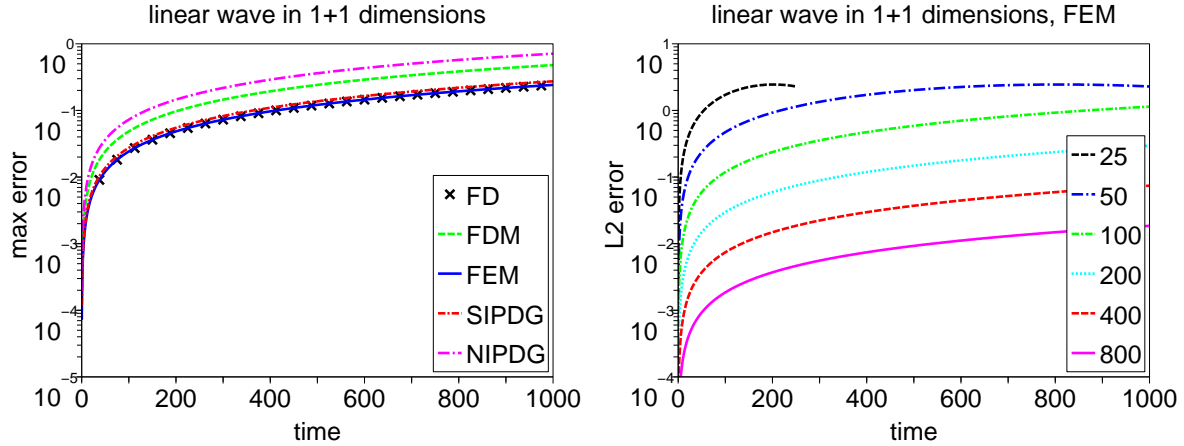


Figure 1. 1+1 linear plane wave: Time evolution of spatial maximum error with $h_1 = 1/200$ (left) and of the l^2 -error of a FEM solution with $n = 1/h$ (right).

4. Applications

4.1. Linear Plane Wave

For illustration purposes, we perform some numerical experiments with the schemes of section 3. The test cases are adapted from the Apples-with-Apples test suite (Alcubierre et al. 2004, Babiuc et al. 2008). We document and compare convergence and stability of the schemes in different settings.

We start with a mono-chromatic traveling plane wave for linearized Einstein's equation (13) and (14) with harmonic gauge (15). We use periodic boundary conditions and a Courant factor $1/2$. The one-dimensional (1+1) test case is defined on the spatial unit interval $(0, 1[$. The exact solution and initial data is $g_{00} = g_{11} = -g_{01} = \sin 2\pi(x_1 - x_0)$. We use an equidistant grid and run all schemes of sections 3.1 to 3.4. Note that the original Apples-with-Apples tests were constructed for non-linear numerical codes, such that very small wave amplitudes effectively ran the codes in the regime of the linearized equations. Standard non-linear solvers like Newton's method in this case reduce the problem to a linear one. Hence, we directly ran a linear code for the linear problem. This is why we can use arbitrary amplitudes of the solution rather than very small ones (Alcubierre et al. 2004).

In figure 1 the time evolution of the spatial maximum error at the grid points for a resolution of $h_1 = 1/200$ is depicted for the FD, FDM, FEM, SIPDG and NIPDG. We use penalty parameters $c_{p0} = 1$ and $c_{p1} = 2$ for SIPDG. Note that continuous error norms like $L_2(0, 1)$ more natural for FEM show a similar behavior with exception of the very first time steps, where an additional interpolation error is added to the global error. The point-wise divergence is bounded, although we do not take any measures to control it. This does not seem to be necessary. The solution in figure 2 (left) shows the spatial errors at the final time $x_0 = 1000$. We see mainly dispersion and the phase error of the different schemes, no errors in the amplitude. This is why the error in fact even

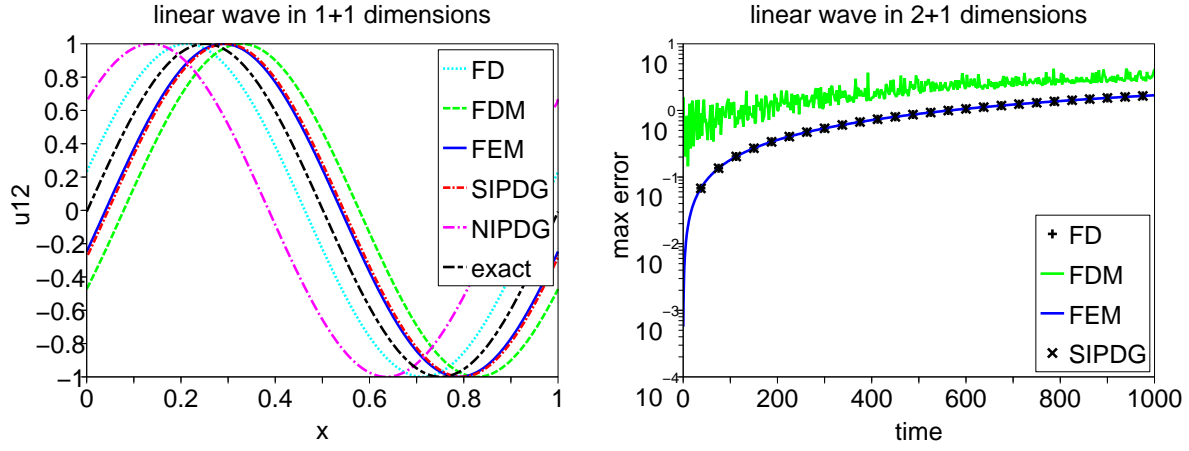


Figure 2. Solution of a linear plane wave in 1+1 for $h_1 = 1/200$ at final time $x_0 = 1000$ (left). Evolution of the maximum error of a wave in 2+1 on a cartesian grid with $h_1 = 1/100$ (right).

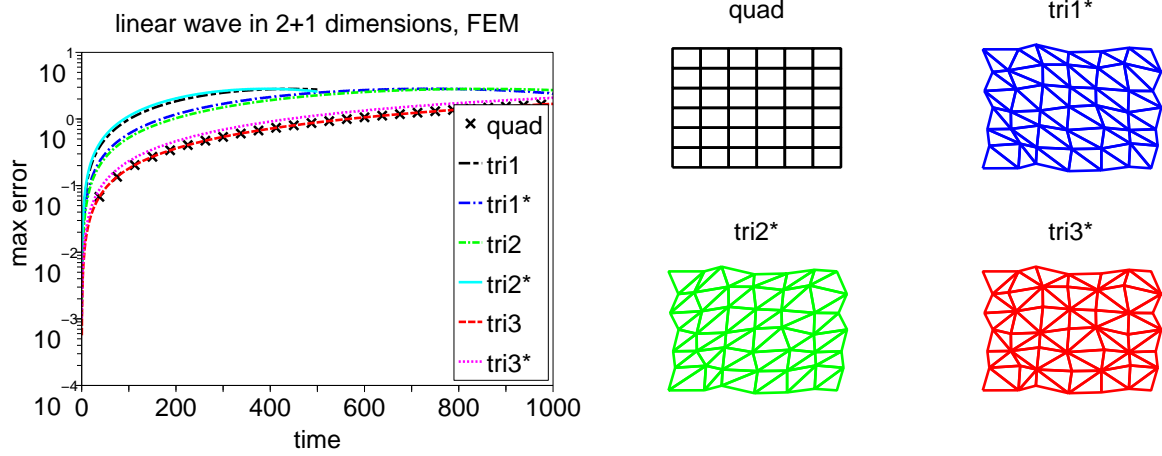


Figure 3. Linear plane wave in 2+1 on some triangulations with $h_1 = 1/100$: evolution of the maximum error (left) and corresponding spatial grids (right).

decreases after some time, see figure 1 (right) $n = 25$ and $n = 50$. We observe a second order convergence of the error, the phase error and the divergence in h_1 for all schemes.

The two-dimensional (2+1) test case is defined on the spatial unit square $(0, 1)^2$ with periodic boundary conditions. The exact solution and initial data is $g_{01} = g_{02} = g_{12} = \sin 2\pi(x_1 + x_2 - \sqrt{2}x_2)$, $g_{11} = g_{22} = (\sqrt{2} - 1)g_{01}$, and $g_{00} = \sqrt{2}g_{01}$. We run all schemes on cartesian equidistant grids, see figure 2 (right), except for the NIPDG scheme for a lack of stability. The SIPDG penalty term is chosen as $c_e = 1/2$, more precisely $\frac{c_p}{|e_{ij}|c_e} = 1/h_0$. The second order convergence is comparable to the 1 + 1 case.

In order to test the dependence on the spatial grid, we run the FEM also on a number of triangular grids, both uniform (tri) and randomly distorted (tri*), see figure 3. Now we obtain a strong dependence of the error on the orientation of the elements. The longest element edges tangential to the direction of the wave leads to a larger approximation error than in normal direction or for quadratic elements.

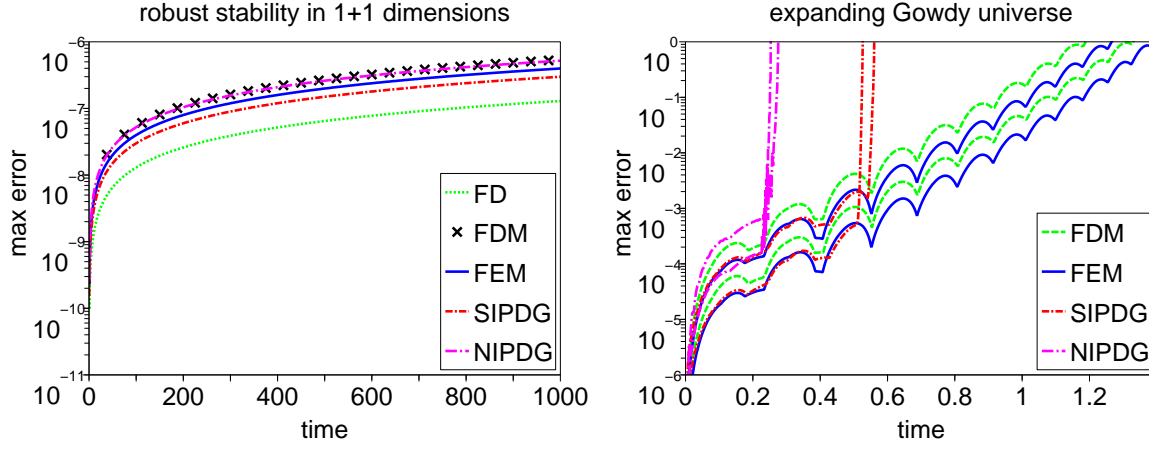


Figure 4. Evolution of the maximum error of the linear robust stability test in 1+1 for $h_1 = 1/200$ (left) and of a non-linear Gowdy wave in 1+1 for $h_1 = 1/100$ and $h_1 = 1/200$ (right).

4.2. Robust Stability Test for Linear Waves

Now we consider a stability test for the linear wave equation. The starting point is a random perturbation of the zero solution. We use periodic boundary conditions on $(0, 1[$, equal distributed $[-\epsilon, \epsilon]$ random values for all initial data, with $\epsilon := 2.5 \cdot 10^{-7} (h_3)^2$ according to (Alcubierre et al. 2004). In figure 4 (left) we observe stability of all schemes with oscillatory solutions for NIPDG and compact stencil FDM.

4.3. Nonlinear Polarized Waves in the Expanding Gowdy Universe

The polarized Gowdy spacetime on the Torus T^3 is a model for a gravitational wave in an expanding universe (Gowdy 1971, New et al. 1998). We use periodic boundary conditions on the spatial unit interval $(0, 1[$ in x_3 direction. The solution is constant along x_1 and x_2 direction. Since we use harmonic gauge, time axis x_0 differs from (Alcubierre et al. 2004). We use a Courant factor $1/4$. The solution $g_{\mu\nu}$ is given by

$$\begin{aligned}
 g &= \text{diag}(-e^{(\lambda+3x_0)/2}, e^{x_0+p}, e^{x_0-p}, e^{(\lambda-x_0)/2}) \text{ with} \\
 p &:= J_0(2\pi e^{x_0})\cos(2\pi x_3) \text{ and} \\
 \lambda &:= -2\pi e^{x_0} J_0(2\pi e^{x_0}) J_1(2\pi e^{x_0}) \cos^2(2\pi x_3) - 2\pi J_0(2\pi) J_1(2\pi) \\
 &\quad + 2(\pi e^{x_0})^2 (J_0^2(2\pi e^{x_0}) + J_1^2(2\pi e^{x_0})) - \frac{1}{2}(2\pi)^2 (J_0^2(2\pi) + J_1^2(2\pi))
 \end{aligned}$$

We run schemes of section 3.6 with 3rd order Gauss quadrature (two points in each coordinate direction) on an element. The SIPDG penalty terms are chosen as $c_{p0} = .5$ and $c_{p1} = 2$. In figure 4 (right) we see the error for spatial resolutions $h_1 = 1/100$ and $h_1 = 1/200$, which demonstrates second order convergence. The DG methods do not seem to be as stable as the others. However, many numerical schemes start to diverge at some time t due to the exponential growth of some of the solution components (Alcubierre et al. 2004).

Conclusion

We have developed new spacetime Finite Element (FEM) and Interior Penalty Discontinuous Galerkin (SIPDG and NIPDG) schemes for second order symmetric hyperbolic wave equations. The Discontinuous Galerkin schemes are computationally more efficient, but require more memory than FEM and Finite Differences methods. A variational formulation of Einstein's equation in harmonic gauge was derived, based on up to first derivatives of solution and trial functions. This led to new Galerkin schemes for numerical relativity. The schemes were presented and tested for second order accurate Galerkin schemes with multi-linear functions and global time steps. The Gowdy wave test demonstrated the need for additional numerical stabilization. This might be obtained by spatial filtering, artificial viscosity, or streamline diffusion.

Extensions to arbitrary spacetime grids or (adaptive) local grid refinement in spacetime are straightforward, but may lead to larger and more expensive to solve equation systems. Higher order polynomials or other more accurate (spectral) function spaces improve the spatial accuracy of the schemes. However higher order in time schemes are more difficult to construct.

Acknowledgments

The author wants to thank G. Schäfer for several hints to the literature. Furthermore, helpful comments by S. Husa and the anonymous referees are acknowledged. This work was partially supported by DFG grant SFB/TR7 "gravitational wave astronomy".

References

- Ainsworth M, Monk P & Muniz W 2006 *J. Scient. Comp.* **27**, 5–40.
- Aksoylu B, Bernstein D, Bond S & Holst M 2008. arXiv:0801.3142v3.
- Alcubierre M, Allen G, Bona C, Fiske D, Goodale T, Guzman F S, Hawke I, Hawley S H, Husa S, Koppitz M, Lechner C, Pollney D, Rideout D, Salgado M, Schnetter E, Seidel E, Shinkai H, Szilágyi B, Shoemaker D, Takahashi R & Winicour J 2004 *Class. Quant. Grav.* **21**, 589.
- Anderson M & Kimn J H 2007 *J. Comp. Phys.* **226**, 466–476.
- Arnold D N, Mukherjee A & Pouly L 1998 in D. F Griffiths, D. J Higham & G. A Watson, eds, 'Numerical Analysis 1997' Addison Wesley Longman pp. 1–15.
- Arnowitt R, Deser S & Misner C W 1962 in L Witten, ed., 'Gravitation: An Introduction to Current Research' Wiley chapter 7, pp. 227–265.
- Babiuc M C, Husa S, Alic D, Hinder I, Lechner C, Schnetter E, Szilágyi B, Zlochower Y, Dorband N, Pollney D & Winicour J 2008 *Class. Quant. Grav.* **25**, 125012.
- Baker G A & Bramble J H 1979 *RAIRO Anal. Numer.* **13**, 75–100.
- Baker J G, Centrella J, Choi D I, Koppitz M & van Meter J 2006 *Phys. Rev. Lett.* **96**, 111102.
- Baumgarte T W & Shapiro S L 1999 *Phys. Rev. D* **59**, 024007.
- Bonazzola S, Gourgoulhon E, Grandclement P & Novak J 2004 *Phys. Rev. D* **70**, 104007.
- Boyle M, Brown D A, Kidder L E, Mroue A H, Pfeiffer H P, Scheel M A, Cook G B & Teukolsky S A 2007 *Phys. Rev. D* **76**, 124038.
- Brandt S & Bruegmann B 1997 *Phys. Rev. Lett.* **78**, 3606–3609.
- Bruhat Y 1962 in L Witten, ed., 'Gravitation: An Introduction to Current Research' Wiley pp. 130–168.

- Campanelli M, Lousto C O, Marronetti P & Zlochower Y 2006 *Phys. Rev. Lett.* **96**, 111101.
- Cohen G C 2002 *Higher-Order Numerical Methods for Transient Wave Equations*. Springer.
- Dupont T 1973 *SIAM J. Numer. Anal.* **10**(5), 880–889.
- Eriksson K, Johnson C & Thomée V 1985 *RAIRO M.M.A.N.* **19**, 611–643.
- Field S E, Hesthaven J S & Lau S R 2009. arXiv:0902.1287.
- Fock V 1959 *The Theory of Time Space and Gravitation*. Pergamon Press.
- French D A & Peterson T E 1996 *Math. Comp.* **65**, 491–506.
- Friedrich H & Rendall A D 2000 *Lect. Notes Phys.* **540**, 127–224.
- Gowdy R H 1971 *Phys. Rev. Lett.* **27**, 826–829.
- Grote M, Schneebeli A & Schötzau D 2006 *SIAM J. Numer. Anal.* **44**, 2408–2431.
- Hulbert G M & Hughes T J R 1990 *Comput. Meth. Appl. Mech. Engin.* **84**, 327–348.
- Jamet P 1978 *SIAM J. Numer. Anal.* **15**, 912–928.
- Metzger J 2004 *Class. Quant. Grav.* **21**, 4625–4646.
- Monk P & Richter G R 2005 *J. Scient. Comp.* **22–23**, 443–477.
- Nedelec J C 1980 *Numer. Math.* **35**, 315–341.
- Nedelec J C 1986 *Numer. Math.* **50**, 57–81.
- New K C B, Watt K, Misner C W & Centrella J M 1998 *Phys. Rev. D* **58**, 064022.
- Pretorius F 2005 *Class. Quant. Grav.* **22**, 425–452.
- Regge T 1961 *Nuovo Cimento A* **19**, 558–571.
- Reula O A 1998 *Living Rev. Relativity* **1**(3), 1–40.
- Rivière B 2008 *Discontinuous Galerkin Methods for Solving Elliptic and Parabolic Equations*. SIAM.
- Shibata M & Nakamura T 1995 *Phys. Rev. D* **52**, 5428–5444.
- Sopuerta C F, Sun P, Laguna P & Xu J 2006 *Class. Quant. Grav.* **23**, 251–285.
- Sorkin R 1975 *Phys. Rev. D* **12**(2), 385–396.
- Straumann N 2004 *General Relativity*. Springer.
- York, Jr. J W 1979 in L. L Smarr, ed., ‘Sources of Gravitational Radiation’ Cambridge Univ. Press pp. 83–126.